DOI:10.1021/jf902580f

JOURNAL OF AGRICULTURAL AND FOOD CHEMISTRY
ARTICLE

Investigation of Thermal Denaturation of Barley Nonspecific Lipid Transfer Protein 1 (ns-LTP1b) by Nuclear Magnetic Resonance and Differential Scanning Calorimetry

Michaela Matejková,[†,∥] Jitka Žídková,[§,∥] Lukáš Žídek,*[,†]
Michaela Wimmerová,[†,‡] Josef Chmelík,[§,⊥] and Vladimír Sklenář[†]

[†]National Centre for Biomolecular Research and [‡]Department of Biochemistry, Faculty of Science, Masaryk University, Kotlářská 2, 611 37 Brno, Czech Republic, and [§]Institute of Analytical Chemistry, Academy of Sciences of the Czech Republic, v.v.i., Veveří 97, 602 00 Brno, Czech Republic. [∥]M.M. and J.Ž. contributed equally to this work. [⊥]Deceased July 16, 2007

The process of thermal denaturation of a covalently modified form of barley grain nonspecific lipid transfer protein 1b (ns-LTP1b) was investigated by nuclear magnetic resonance (NMR) and differential scanning calorimetry up to 115 °C. The denaturation was found to be irreversible and highly cooperative. A method of numerical quantitative analysis allowing us to fit the NMR data to a transition state model without further simplification was developed. On the basis of the obtained values of transition state enthalpy and entropy, the rate of denaturation was calculated as a simple measure of protein stability at various temperatures. The effect of disulfide bond reduction on thermal denaturation of ns-LTP1b was studied and discussed in the context of quality control of barley products during storage and processing.

KEYWORDS: Nonspecific lipid transfer protein 1; barley grain; thermal denaturation; nuclear magnetic resonance; differential scanning calorimetry

INTRODUCTION

Nonspecific lipid transfer protein 1 (ns-LTP1) is an ubiquitous plant protein able to transfer lipids between membranes in vitro. Properties of ns-LTP1 were recently reviewed by Gorjanović (*1*). ns-LTP1 is present in cereal seeds, where it accounts for 5−10% of total soluble proteins. Barley ns-LTP1 is a basic protein (pI ≈ 9) consisting of 91 amino acid residues (molecular mass of 9695 Da in the reduced state). As other plant ns-LTP1s, its compact fold comprises four α-helices and a C-terminal arm. The structure is stabilized by four disulfide bridges (*2*). The protein has a hydrophobic cavity allowing binding of different types of lipids (*3*−*5*). Moreover, an isoform of covalently modified lipid transfer protein 1b (ns-LTP1b), isolated from barley grain, contains a lipidlike molecule of 294 Da as a postranslational modification (*6*, *7*), which has been identified as a reactive oxylipin [α-ketol of 9-hydroxy-10-oxo-12(*Z*)-octadecenoic acid] produced in barley seeds by oxygenation of linoleic acid followed by dehydration of the resulting hydroperoxide (*8*). Physiological roles of ns-LTP1 in cutin synthesis (*5*) and protection against heavy metals (*9*, *10*) have been proposed, and the antimicrobial activity of ns-LTP1 has been documented (*11*). In addition, ns-LTP1 is extremely heat- and protease-resistant (*12*), survives the procedure of making beer, is present in beer, and has an effect on foaming (*13*).

The importance of the unusual heat stability of ns-LTP1 was soon recognized. Lindorff-Larsen and Winther (*14*) investigated the stability of the lipid-modified ns-LTP1b toward denaturants, proteases, and temperature up to 100 °C. Their DSC data showed a melting temperature well above 100 °C, in good agreement with no major structural changes observed when monitoring native fluorescence of ns-LTP1b in a range of 20−90 °C. Great attention has been paid to the thermal changes of ns-LTP1 isoforms during the process of brewing. Jégou et al. studied the thermal denaturation of ns-LTP1 during the malting process (*15*). Van Nierop et al. investigated the effect of heat denaturation of ns-LTP1 on the beer foam quality (*16*) and characterized partially and completely denatured ns-LTP1 (using a sample containing approximately 30% ns-LTP1b) by a variety of techniques. ns-LTP1b was also one of the heat-stable proteins described in barley grain, malt, and beer in a comparative proteomics study by Perrocheau et al. (*17*). The effects of the lipid modification, glycation, and reduction of disulfide bonds on the heat stability of ns-LTP1 were recently addressed in a detailed study by Perrocheau et al. (*12*).

In spite of the number of thermal stability studies reported in the literature, two issues remain to be addressed to understand the impact of the thermal denaturation of ns-LTP1 during brewing and other processes involving heating of barley and other grain products. First, the ns-LTP1b denaturation curves were so-far published only up to 100 °C. However, Van Nierop et al. (*16*) reported dramatic differences in the extent of ns-LTP1 denaturation among samples incubated for 60 min at 96, 105, and 110 °C. The second and probably more important issue is the proper description of irreversibility of the thermal denaturation of ns-LTP1b. While reversible denaturation curves can be interpreted in terms of van't Hoff enthalpy ΔH and of melting temperature T_m directly related to the entropy ΔS of unfolding ($T_m = \Delta H/\Delta S$),

*To whom correspondence should be addressed. E-mail: lzidek@chemi.muni.cz.

 Published on Web 08/31/2009

such an approach is not relevant for irreversible denaturation (*18*). Accordingly, a thermodynamic description was avoided in the literature cited above, and raw data were presented. It should be noted that the melting temperatures derived from the reported irreversible temperature curves are not thermodynamic constants (as in the case of the reversible unfolding), since the measured T_m values depend on the rate of heating.

Here, we present a study of thermal denaturation of ns-LTP1b in a wide temperature range, up to 120 °C, and interpret the data in a context of an appropriate kinetic model. Its results allowed us to express the half-life of the protein at various temperatures as a simple measure of its stability. The effects of reducing agents and implications for quality of barley products during storage and processing are also discussed.

MATERIALS AND METHODS

Theoretical Model of Denaturation. The kinetic model used in this study describes denaturation as an irreversible conversion of the native state N into the unfolded state U. Applicability of such a model to the in principle multistep process of denaturation is discussed in the literature (*19*). The denatured fraction of the protein $x = [U]/([U] + [N])$ can be obtained by solving the differential equation

$$\frac{d(1-x)}{dt} = -k(1-x) \quad (1)$$

where t is time and k is the first-order rate constant (*18*, *20*). The temperature dependence of the rate constant can be expressed in terms of the theory of the activated complex as

$$k = \frac{k_B T}{h} e^{-(\Delta H^{\ddagger} - T\Delta S^{\ddagger})/RT} \quad (2)$$

where k_B is the Boltzmann constant, R is the universal gas constant, h is the Planck constant, T is the thermodynamic temperature, and $\Delta H^{\ddagger}$ and $\Delta S^{\ddagger}$ are enthalpy and entropy of the transition state (*21*), respectively. The solution of eq 1 will be discussed for two cases, for a series of isothermal steps and for a linear temperature increase with a constant rate $v = dT/dt$.

If the temperature T does not change in a time interval $\Delta t_1 = t_1 - t_0$, eq 1 has a simple solution $x_1 = 1 - (1 - x_0)\exp(-k\Delta t_1)$. Therefore, the fraction of the unfolded protein after n steps of incubation at various temperatures T_n is given by

$$x_n = 1 - e^{-\sum_{j=1}^{n} k_j \Delta t_j} \quad (3)$$

where k_j is the first-order rate constant at the j-th temperature T_j.

The average value of x during the interval (t_{n-1},t_n) can be obtained by integration

$$\langle x \rangle_{t_{n-1},t_n} = \frac{1}{t_n - t_{n-1}} \int_{t_{n-1}}^{t_n} x(t)\, dt$$

$$= 1 - \frac{e^{-\sum_{j=1}^{n-1} k_j \Delta t_j}}{t_n - t_{n-1}} \int_{t_{n-1}}^{t_n} e^{-k_n(t - t_{n-1})}\, dt = 1 - e^{-\sum_{j=1}^{n-1} k_j \Delta t_j} \frac{1 - e^{-k_n \Delta t_n}}{k_n \Delta t_n} \quad (4)$$

If the temperature increases with a constant rate v, eq 1 can be converted into a differential equation describing the temperature dependence $dx/dT = k\,(1 - x)/v$. This equation has a general solution

$$x(T) = 1 - e^{-\int_{T_0}^{T} [k(T)/v] dT} \quad (5)$$

where T_0 is the initial temperature. Differentiation of this equation provides

$$\frac{dx(T)}{dT} = \frac{k(T)}{v} e^{-\int_{T_0}^{T} [k(T)/v] dT} \quad (6)$$

The inflection point of the temperature dependence of x can be derived from the equation $d(1 - x)/(1 - x)\, dT = -k/v$ (*20*). Differentiation of the right-hand side, defined by eq 2, gives

$$\frac{d^2 \ln(1-x)}{dT^2} = -\frac{k_B T}{hv}\left(1 + \frac{\Delta H^{\ddagger}}{RT}\right) e^{-(\Delta H^{\ddagger} - T\Delta S^{\ddagger})/RT} \quad (7)$$

Application of the chain rule to the left-hand side results in

$$\frac{d^2 \ln(1-x)}{dT^2} = \frac{1}{1-x}\frac{d^2(1-x)}{dT^2} - \frac{1}{(1-x)^2}\left[\frac{d(1-x)}{dT}\right]^2 \quad (8)$$

Combining eqs 7 and 8 and setting $d^2(1 - x)/dT^2 = 0$ leads to the definition of the apparent denaturation temperature T_m:

$$\left(-\frac{\Delta H^{\ddagger}}{RT_m} + \frac{\Delta S^{\ddagger}}{R}\right) + \ln \frac{k_B T_m^2}{hv} = \ln\left(1 + \frac{\Delta H^{\ddagger}}{RT_m}\right) \quad (9)$$

In the relatively narrow range of denaturation temperatures observed for a particular protein, temperature variations of the right-hand side of eq 9 can be neglected, and the activation enthalpy can be calculated from T_m values obtained at different heating rates v:

$$\Delta H^{\ddagger} = \ln \frac{v_1 T_{m2}^2}{v_2 T_{m1}^2}\left(\frac{1}{T_{m1}} - \frac{1}{T_{m2}}\right)^{-1} \quad (10)$$

Ns-LTP1b Isolation and Characterization. Barley grains (*Hordeum vulgare* cv. Jersey) were milled, and proteins were extracted from 0.5 kg of the flour in 1.2 L of deionized water for 5 h by stirring gently at room temperature. Extracts were centrifuged, and 66 mL of 200 mM 4-morpholinoethanesulfonic acid (MES) buffer, pH 6, was added to 600 mL of supernatant. This solution was loaded onto a laboratory-made cation exchange column packed with Streamline SP (Amersham Biosciences, Uppsala, Sweden). Proteins were eluted with a step gradient ranging from 0 to 700 mM NaCl with 10 steps of 60 mL. Fractions were collected and analyzed by sodium dodecylsulfate−polyacrylamide gel electrophoresis (SDS-PAGE) and matrix-assisted laser desorption/ionization time-of-flight mass spectrometry (MALDI-TOF MS). The fractions containing proteins with a molecular mass around 10 kDa were pooled and lyophilized. The dry material was dissolved in 20 mM ammonium acetate and 0.05% sodium azide and applied onto a gel permeation column (102 cm × 0.95 cm) packed with Sephadex G-50 (Sigma-Aldrich, St. Louis, MO). The fractions containing proteins of mass close to 10 kDa were collected, analyzed by SDS-PAGE and MALDI-TOF MS, and lyophilized. For the heat denaturation studies, the samples were dissolved to the final concentration in 10 mM acetate, 0.5 mM sodium azide, and 10% (v/v) deuterium oxide, pH 4.0 (adjusted with HCl, without correction for the isotopic effect). Dispersity of the sample before and after the experiment was determined by dynamic light scattering (DLS) measurements at 25 °C on a DynaPro Plate Reader (Wyatt Technology Corp., Germany). The protein concentration was determined spectrophotometrically at 280 nm, using an absorption coefficient of 4600 M^{-1} cm^{-1} (*3*).

Mass Spectrometry. Samples were prepared by mixing 1 μL of ns-LTP1 solution with 1 μL of ProMix2 calibration mixture (LaserBio Laboratories, Sophia-Antipolis Cedex, France) and 2 μL of matrix solution, containing 10 mg/mL sinapinic acid in acetonitrile:0.1% trifluoracetic acid (1:1 v/v). The mass spectra were measured on 4700 Proteomics Analyzer (Applied Biosystems, Framingham, MA) equipped with a Nd:YAG laser (355 nm) of < 500 ps pulse and a 200 Hz firing rate. MS data were internally calibrated using horse heart cytochrome *c* and horse heart myoglobin peaks.

Nuclear Magnetic Resonance (NMR) Spectra Acquisition, Processing, and Analysis. One-dimensional proton spectra monitoring the thermal denaturation of 0.1 mM ns-LTP1 in the temperature range from 37 to 115 °C were measured in 5 mm WILMAD screw-cap NMR tubes (Wilmad-LabGlass, Buena, NJ) on a 500 MHz Bruker Avance NMR spectrometer (Bruker Biospin, Karlsruhe, Germany), equipped with a direct QNP probehead. The choice of the NMR probehead was given by its high temperature limit. The measurements were performed in regular time intervals (25 min for each temperature step). The temperature was

calibrated with the ethylene glycol:d_6-dimethyl sulfoxide (4:1 v/v) mixture (New Era, Vineland, NJ), using a calibration curve provided by Bruker Biospin. In each spectrum, 512 scans were recorded with 4096 complex points, with a spectral width of 8013 Hz and with the proton carrier placed at the resonance of water. The solvent peak was suppressed by presaturation. The solvent signal was filtered out, and the data were apodized with a cosine-square function, zero-filled to 65536 points, Fourier transformed, and phased, and a third-order baseline correction was applied. Software NMRPipe (*22*) was used for spectra processing. Proton chemical shifts in the lowest temperature spectrum were referenced to 2,2-dimethylsilapentane-5-sulfonic acid (*23*). Spectra recorded at higher temperatures were frequency shifted so that the methyl peak of acetate overlapped in all spectra.

Effects of temperatures in a range from 33 to 70 °C were also monitored by running one-dimensional (1D) proton spectra and two-dimensional (2D) ^{1}H−^{1}H nuclear Overhauser effect spectroscopy (NOESY) spectra (*24*) on a 600 MHz Bruker Avance NMR spectrometer (Bruker Biospin), equipped with an inverse QXI probehead. The ns-LTP1b concentrations of 0.055 and 1 mM were used in 1D and 2D experiments, respectively. In 1D spectra, 256 scans were recorded with 8192 complex points, with a spectral width of 9615 Hz, and with the proton carrier placed at the resonance of water. The spectra were processed and analyzed as described above. The 2D NOESY spectra were acquired with the mixing time of 120 ms, with the spectral width of 12 ppm in both dimensions, and with 2048 and 300 complex points in the direct and indirect dimension, respectively. The spectra were zero-filled to 2048 points in both dimensions and processed in a similar fashion as the 1D spectra.

Methyl resonances of ns-LTP1 were used to monitor spectral changes of the protein during heating. Intensities and chemical shifts of individual methyl groups were measured in 2D spectra and for well-resolved peaks also in the 1D spectra. To improve precision of the data, the following procedure of quantitating spectral changes has been adopted. A difference spectrum between the given spectrum and the spectrum recorded at the lowest temperature was calculated, and the absolute value of the difference spectrum was integrated in a region from 0.70 to 0.95 ppm.

The integral of the absolute value difference spectra Y was fitted to the equation

$$Y_n = (a_0 + b_0 T_n) + [a_1 - a_0 + (b_1 - b_0) T_n]\langle x\rangle_n \quad (11)$$

where coefficients a_0, b_0, a_1, and b_1 describe temperature changes of spectra of the native and denatured forms (assumed to be linear) and $\langle x\rangle_n$ is the average ratio of the denatured protein in the n-th temperature step. As the NMR spectra were not recorded through the whole period Δt_n but the data acquisition started at $t_a > t_{n-1}$, after a delay necessary to stabilize temperature and to shim and wobble the spectrometer, eq 4 had to be slightly modified to define $\langle x\rangle_n$. Integration of $x(t)$ started at t_a, giving

$$\langle x\rangle_n \equiv \langle x\rangle_{t_a, t_n} = 1 - e^{-\sum_{j=1}^{n} k_j \Delta t_j} \frac{e^{k_n \Delta t_a} - 1}{k_n \Delta t_a} \quad (12)$$

where Δt_a is the acquisition time.

Parameters a_0 and b_0 were adjusted together with $\Delta H^{\ddagger}$ and $\Delta S^{\ddagger}$ during fitting to eq 11, while a_1 and b_1 were determined separately by fitting values of Y_n obtained during repeated heating of already denatured sample to the linear equation $Y_n = a_1 + b_1 T_n$. Levenberg−Marquardt nonlinear regression of the data was programmed in OCTAVE (J. W. Eaton et al., University of Wisconsin, OCTAVE 2.1.71) (http://www.gnu.org/software/octave/). The described approach based on the numeric fitting to eq 4 allowed us to avoid approximations used in earlier works (*18*, *20*), in which the temperature dependence of the rate constant k was expressed as a truncated Taylor series.

NMR Heating Experiments. The following setups were used to study the effect of heating: NMR experiment 1, 2D NOESY spectra were recorded in regular intervals of 20 h 40 min at 33, 42, 51, 60, 69, 51, and 33 °C. NMR experiment 2, temperature was gradually increased by 5.6 K increments in 25 min steps from 37 to 115 °C, and a 1D spectrum was acquired at each temperature. NMR experiment 3, 1D spectra were recorded at 37, 59, and 81 °C in 30 min intervals, and then, the temperature was incremented by 3.4 K in 30 min steps, and a 1D spectrum was taken at each temperature. NMR experiment 4, 1D spectrum was taken at the beginning, after 10 min and after 150 min of incubation at 100 °C. All spectra were measured at 33 °C. NMR experiment 5, 10 mM $Na_2S_2O_5$ was added to the sample, the temperature was increased in 30 min steps from 33 to 70 °C in increments of 4.5 K, and a 1D spectrum was taken at each temperature. To achieve complete denaturation, additional 1D spectra were taken in 30 min intervals at 60 °C. NMR experiment 6, 2 mM $Na_2S_2O_5$ was added to the sample, and the same protocol was applied as in NMR experiment 2. NMR experiment 7, 30 mM reduced glutathione (GSH) was added, and 1D spectra were recorded repeatedly at 60 °C for 64 h (12 spectra were taken, the first one immediately prior to the glutathione addition).

Differential Scanning Calorimetry (DSC). DSC experiments were performed on a VP-DSC MicroCalorimeter (MicroCal, Inc., Century City, CA) with cell volumes of 0.5 mL. The temperature resolution was ±0.1 °C. All solutions were degassed before measurements. The scans ran from 10 to 130 °C at the scan rate of 60 °C/h. The experiments were performed at a protein concentration of 0.1 mM in 10 mM ammonium acetate, 0.5 mM sodium azide, and 10% (v/v) deuterium oxide, pH 4.0 (adjusted with HCl). Reference baseline was obtained by buffer vs buffer scan and subtracted from the measured data.

The heat capacity C_p can be defined as $Q\,dx/dT$ (*18*, *20*), where Q is the total heat consumed during the process. The calorimetric curve obtained in this study was treated as a sum of M heat capacity peaks

$$C_p = \sum_{j=0}^{M} C_{p,j} \quad (13)$$

The peak at the highest temperature was defined according to eq 6 as

$$C_{p,0} = Q_0 \frac{k_0(T)}{v} e^{-\int_{T_0}^{T} [k_0(T)/v]dT} \quad (14)$$

while the other peaks were used to account for the asymmetry of the denaturation curve. They were described either as irreversible transitions

$$C_{p,j} = Q_j \frac{k_j(T)}{v} e^{-\int_{T_0}^{T} [k_j(T)/v]dT} \quad (15)$$

or by the equation of a reversible transition (*19*):

$$C_{p,j} = Q_j \frac{\Delta H_j}{k_B T^2} \frac{e^{(\Delta H_j - T\Delta S_j)/k_B T}}{[1 + e^{(\Delta H_j - T\Delta S_j)/k_B T}]^2} \quad (16)$$

The following models were used to fit the calorimetric curve (**Table 2**): model 1, fitting only the major peak to eq 14; models 2 and 3, fitting data to one irreversible (eq 14) and one or two reversible (eq 16) transitions, respectively; and models 4 and 5, fitting data to two or three irreversible transitions (eqs 14 and 15), respectively.

Values of $\Delta H_j^{\ddagger}$ and $\Delta S_j^{\ddagger}$ defining $k(T)$ of the irreversible transition(s), together with values of Q_j, ΔH_j, and ΔS_j describing the reversible transition(s) were fitted by the nonlinear regression programmed in OCTAVE as described above. The value of the heat absorbed during the highest temperature transition (Q_0) was fixed to the difference between the total heat Q obtained by integration of the calorimetric curve and the sum of heats Q_j fitted for the other transitions [$Q_0 = Q - (Q_1 + ... + Q_{M-1})$].

RESULTS

Characterization of Prepared ns-LTP1b. The native ns-LTP1b was purified according to Jégou (*25*). The freshly prepared sample was almost completely covalently modified with 9-hydroxy-10-oxo-12(*Z*)-octadecenoic acid, as revealed by quantitative analysis of its 1D ^{1}H NMR spectrum [the determined lipid:protein ratio was 0.92 ± 0.05 and was qualitatively confirmed by MALDI-TOF MS (see Figure S1A in the Supporting Information)]. The determined molecular mass of the protein (9982.5 ± 0.3) was identical to the mass of ns-LTP1b (9983 kDa) reported by Perrocheau et al.(*12*) and close to the value calculated from the

sequence (9980.9). The mass distribution from the DLS measurements showed that 99.9% of mass of the native sample corresponded to a particle average size of 1.7 nm, giving a molecular mass of 10 kDa.

Reversible Thermal Changes of Native ns-LTP1b. Reversible effects of heating were studied by running 2D ^{1}H NOESY NMR spectra at various temperatures up to 70 °C (NMR experiment 1). The amide proton chemical shifts moved upfield with increasing temperature (on average by approximately −5 ppb per Kelvin). The aliphatic protons exhibited much smaller chemical shift changes. These results confirmed that the protein structure does not change significantly in the studied temperature range. The decreasing amide proton chemical shifts reflected weakening hydrogen bonds at higher temperatures (*26*). Chemical shift changes of the aliphatic protons were small and did not exhibit any systematic trend, indicating that the protein structure remained intact in the tested temperature range (*26*). The chemical shifts and intensities of most peaks in a spectrum measured after cooling down the sample to the original temperature were very close to the values measured before the heating. Peaks of the oxylipin modification represented a notable exception. The intensity of the well-resolved signal of H12 of the lipid decreased to 45% of its original value when the sample was cooled down. It documents that the labile ester bond is slowly hydrolyzed at relatively low temperatures, when no denaturation is observed. Fitting the relative intensities of the NOESY peaks (volume of the oxylipin H12−H13 cross-peak normalized with respect to the volume of the Tyr 16 H^{δ}−H^{ε} cross-peak) to eq 12 provided estimation of the hydrolysis rates at various temperatures (5.2×10^{-6} s^{-1} at 70 °C and 1.5×10^{-5} s^{-1} at 96 °C). However, the rate constant values should be interpreted with caution, as possible differences in the temperature dependence of the NOESY peaks were neglected. Nevertheless, the obtained values indicate that the hydrolysis is much slower than the time scale of thermal denaturation experiments used in this study.

The temperature range of monitoring reversible thermal effects was extended close to the denaturation temperature in NMR experiment 2. In the course of the experiment, changes of chemical shifts of well-resolved methyl peaks of Val 75 $H^{\gamma 1}$ and Ile 90 $H^{\delta 1}$ were measured. A linear increase of chemical shift values was observed up to 100 °C with the same slope as determined in experiment 1 (Figure S2 of the Supporting Information). The measured values were compared to random-coil chemical shifts of isoleucine $H^{\delta 1}$ protons (approximately 0.80 ppm) and valine γ protons (approximately 0.84 ppm), estimated from 2D NOESY spectra of denatured ns-LTP1b (not shown). The chemical shift of Ile 90 $H^{\delta 1}$ shifted toward the random coil as the temperature increased with a slope of 1.2 ppb K^{-1}. This could be interpreted as a reversible loosening of the C terminus. On the other hand, much smaller chemical shift changes (with a slope of 0.4 ppb K^{-1}) were observed for Val 75 $H^{\gamma 1}$. Therefore, the central region of ns-LTP1b seems to be well-structured even at elevated temperatures.

Thermal Denaturation of Native ns-LTP1b. Heat denaturation of the native ns-LTP1b was studied by NMR experiments 2−4 and by DSC. NMR experiment 2 allowed us to observe spectral changes in the whole range of the gradually increasing temperature from 37 to 115 °C, however, at a price of recording a relatively few points across the transition. Therefore, the denaturation was followed with a slower temperature increase between 81 and 115 °C in NMR experiment 3. The structural changes related to denaturation were monitored by analyzing the methyl region of the spectra. Methyl groups typically form the hydrophobic core of folded proteins and therefore reflect denaturation most directly (*19*). In addition, signals of methyl groups are most intense and resonate far from the frequency of water. Absolute

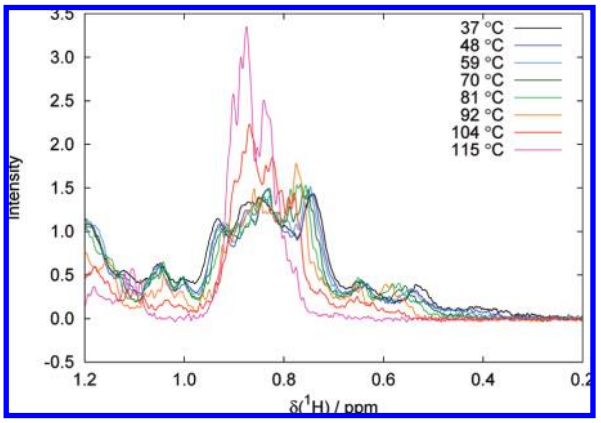

Figure 1. Overlaid NMR spectra of native ns-LTP1b taken in the course of thermal denaturation at temperatures indicated in the legend.

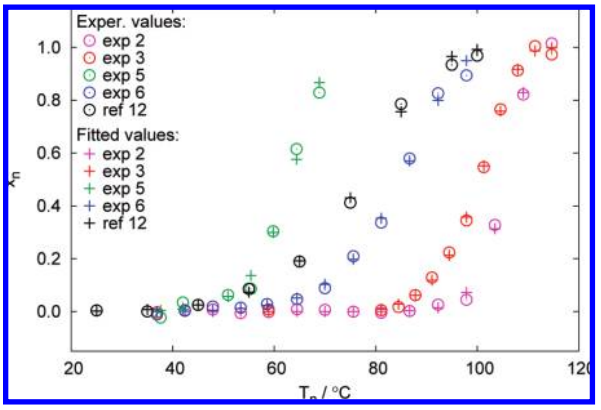

Figure 2. Fraction of the denatured protein *x*, measured as integrals Y_n of the absolute value difference NMR spectra, fitted to the kinetic model in the course of thermal denaturation. Data from NMR experiments 2, 3, 5, and 6 and from ref *12* are displayed and color-coded as indicated in the legend. Circles represent values calculated from the experimental data, while crosses represent values calculated from the fitted kinetic model.

values of the intensity difference, integrated over the whole methyl region of the spectrum, provided a sensitive parameter allowing us to reliably quantitate the spectral changes. Such an approach supplied more reliable data than integration of well-resolved methyl signals as their peak areas were strongly influenced by the baseline definition and a relatively low signal-to-noise ratio.

Transitions to the unfolded state were observed at temperatures higher than 100 °C in both NMR experiments 2 and 3 (**Figure 1**). Spectra taken after cooling the protein were very similar to spectra recorded above the apparent denaturation temperature (Figure S3 of the Supporting Information), revealing the irreversible nature of the denaturation. The integrated absolute values of the intensity difference Y_n were fitted to eq 11 (**Figure 2**). Results of the kinetic analysis are presented in **Table 1**. Values of the activation Gibbs free energy were calculated for 105 °C, which allowed a direct comparison with previously reported results of isothermal denaturation experiment performed at this temperature (*16*).

The activation enthalpy can also be calculated from transition temperatures measured at different heating rates (eq 10). The value of $\Delta H^{\ddagger} = 199$ kJ mol^{-1} was obtained for T_m determined in NMR experiments 2 and 3.

In NMR experiment 4, spectral changes were monitored after cooling down samples incubated at 100 °C, that is, slightly below the transition temperatures determined in NMR experiments 2 and 3.

Table 1. Parameters of the Kinetic Model of Irreversible Denaturation Obtained from the NMR Experiments Reported Here and from Data in Literature

source	c^a (mM)	v (mK s^{-1})	T_m (°C)	$\Delta H^{\ddagger}$ (kJ mol^{-1})	$\Delta S^{\ddagger}$ (kJ mol^{-1} K^{-1})	$\Delta G^{\ddagger}$ (kJ mol^{-1})	r^2
exp 2	0	3.73	105.6 ± 0.2	33 ± 20	0.560 ± 0.053	117.7[b]	0.9992
exp 3	0	1.87	101.6 ± 0.3	191 ± 10	0.193 ± 0.027	117.8[b]	0.9994
ref *16*	0	0[c]	105[d]	NA[e]	NA	118.7	NA
exp 5	10[f]	2.50	64.0 ± 1.9	176 ± 69	0.208 ± 0.205	106.6[g]	0.9912
ref *12*	10[f]	11.11	80.1 ± 1.8	89 ± 17	−0.056 ± 0.048	107.6[g]	0.9983
exp 6	2[f]	3.73	86.2 ± 1.0	119 ± 16	0.016 ± 0.045	113.3[g]	0.9976
exp 7	30[h]	0[c]	60[d]	NA	NA	112.0	NA

[a] Concentration of reducing agent. [b] Calculated for 105 °C. [c] Isothermal incubation. [d] Incubation temperature. [e] Not applicable. [f] Sodium metabisulfite used for reduction. [g] Calculated for 60 °C. [h] GSH used for reduction.

Table 2. Results of Fitting the Heat Capacity Changes during Thermal Denaturation of Native LTP1b Monitored by DSC to Various Models

model	j	transition	Q_j (kJ mol^{-1})	ΔH_j^a (kJ mol^{-1})	ΔS_j^a (kJ mol^{-1} K^{-1})	$\Delta G^{\ddagger}$ (kJ mol^{-1})	r^2
1	0	irreversible[b]	131	165	0.133	114.7[c]	0.9992
2	0	irreversible	188	166	0.137	114.2[c]	0.9951
	1	reversible	158	103	0.287		
3	0	irreversible	100	249	0.353	115.5[c]	0.9964
	1	reversible	119	108	0.304		
	2	reversible	127	188	0.501		
4	0	irreversible	142	196	0.215	114.7[c]	0.9987
	1	irreversible	205	64	−0.130		
5	0	irreversible	130	204	0.235	115.1[c]	0.9992
	1	irreversible	210	68	−0.120		
	2	irreversible	6	158	0.169		

[a] Transition state values (‡) are given for irreversible transitions. [b] Fitted in the temperature range of 105−123 °C only. [c] Calculated for 105 °C.

While only minor changes were observed after 10 min of incubation, approximately 54% ns-LTP1b was denatured after 150 min of incubation, in a good agreement with the rate constant of 1.8×10^{-4} s^{-1} calculated from $\Delta H^{\ddagger}$ and $\Delta S^{\ddagger}$ obtained in NMR experiment 3.

The heat absorbed by the identical ns-LTP1b solution was measured by DSC. The black line in **Figure 3** shows the calorimetric profile of ns-LTP1b in the 10−130 °C temperature range at a scan rate of 16.7 mK s^{-1}. A large endothermic peak was observed with maximum heat absorption around 111 °C. A rescan of the cooled ns-LTP1b samples revealed no denaturation peaks and indicated an irreversible overall denaturation of the protein.

Total heat Q, calculated by integrating the calorimetric curve, was 346 kJ mol^{-1}. The calorimetric curve was fitted to models of multiple transitions, as described in the Materials and Methods. Results of fitting to several reversible and irreversible models of the predenaturation peaks are summarized in **Table 2**. Models 4 and 5, involving one or two irreversible predenaturation steps, provided kinetic parameters very close to those obtained in NMR experiment 3, which sampled the denaturation region of temperatures better than NMR experiment 2. Model 5, fitting the experimental curve best, is presented in **Figure 3**.

The denatured samples were investigated by NMR spectroscopy, mass spectrometry, and DLS. NMR spectra of the denatured protein exhibited features characteristic for unfolded peptides, that is, sharp peaks within a narrow range of frequencies. Integration of the methyl region of the spectrum did not reveal any significant loss of the signal during denaturation (94% of the intensity integrated over the methyl region was recovered). The samples were clear, without macroscopic precipitation. DLS measurements of the sample after denaturation demonstrated behavior similar to the native sample, with a negligible shift of the most distributed particle size to 1.9 nm (corresponding to 12 kDa) and slightly higher dispersity but still showing 98% of the mass corresponding to monomer particle. The major peak in mass spectra of denatured ns-LTPIb ($m/z = 9688.9 \pm 0.8$) was close to

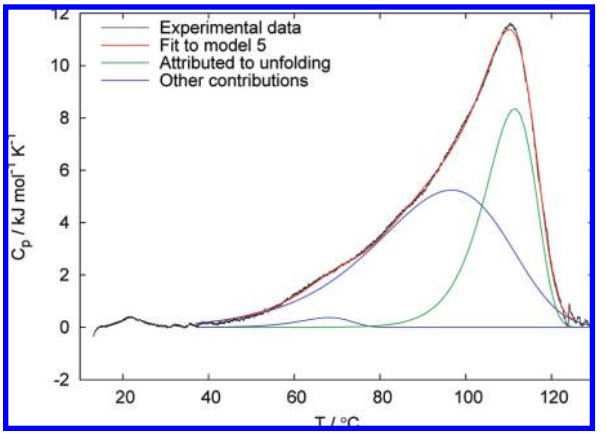

Figure 3. Heat capacity changes monitored by DSC during thermal denaturation of native ns-LTP1b fitted to model 5 described in **Table 2**.

the mass of unmodified ns-LTP1 with disulfide bridges (re)formed (9686.8 Da). The observed hydrolysis of the oxylipin is in a good agreement with the results of NMR experiment 1 and with the data published by Van Nierop et al., showing that no signals of intact ns-LTP1b were observed at the denaturing conditions, that is, after incubation at 110° for 60 min, while only a negligible loss of the modification was observed after incubation at 96° for 60 min (*16*). A peak of comparable intensity at m/z lower by 16.6 ± 0.1 and a less intense peak at m/z lower by 33.9 ± 0.3 were attributed to deamidation (Figure S1B of the Supporting Information).

Reduction of Disulfide Bridges of ns-LTP1b. A large decrease of heat stability and complete denaturation curves were reported for ns-LTP1 isoforms with the disulfide bonds reduced (*12*). Therefore, denaturation of ns-LTP1b was investigated under identical reducing conditions in our study. Disulfide bonds of ns-LTP1 were disrupted by the addition of sodium metabisulfite (*12*) ($Na_2S_2O_5$, final concentration of 2 and 10 mM) or GSH (final

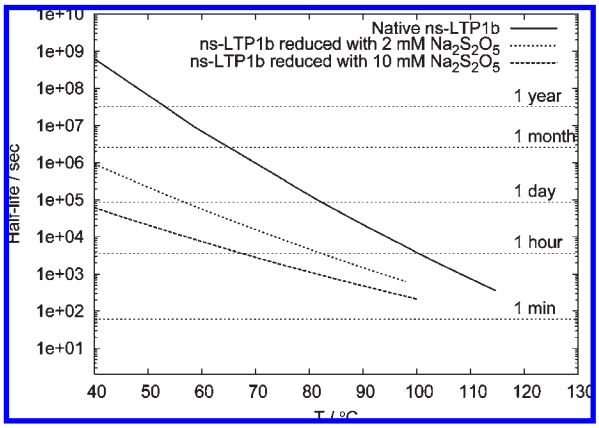

Figure 4. Half-life of native ns-LTP1b (data from NMR experiment 3), ns-LTP1b reduced with 2 mM metabisulfite (data from NMR experiment 6), and ns-LTP1b reduced with 10 mM metabisulfite (data from ref *12*), evaluated for various temperatures based on the transition state enthalpy and entropy values.

concentration of 30 mM). Opening of the disulfide bridges was confirmed by mass spectrometry. Up to three adducts of $\Delta M = 82$, corresponding to the formation of S-sulfonates, were identified in spectra measured immediately after the reduction with $Na_2S_2O_5$. On the other hand, analogous mixed disulfide species of $\Delta M = 307$ were observed only after a long incubation with glutathione or when heating the GSH/ns-LTP1b mixture for 10 min at 60 or 80 °C. To compare the amounts of detected S-sulfonates and mixed disulfides in a semiquantitative manner, a ratio I_2/I_0 was calculated, where I_0 is the peak intensity of ns-LTP1b and I_2 is the peak intensity of ns-LTP1b with two adducts, that is, with half disulfide bonds replaced with the modification. The I_2/I_0 ratios of 0.046 ± 0.006 and 0.55 ± 0.09 were obtained after reduction with 2 and 10 mM metabisulfite, respectively. Heating of ns-LTP1b reduced with 30 mM GSH to 60 and 80 °C resulted in I_2/I_0 ratios of 0.060 ± 0.002 and 0.41 ± 0.11, respectively.

NMR spectra also exhibited slight changes upon reduction. At higher concentrations (1 mM ns-LTP1b and 60 mM GSH), production of GSH was also observed in amounts corresponding to 0.45 and 0.85 equivalents of the protein disulfide bridges after 10 min and 18 h of incubation at 33 °C, respectively.

Thermal Denaturation of Reduced ns-LTP1b. Heat denaturation of ns-LTP1b reduced with sodium metabisulfite was studied using the same approach as applied to the native protein. The effect of 10 mM metabisulfite was tested in NMR experiment 5. The NMR denaturation experiment was also repeated with the concentration of the reducing agent lowered to 2 mM (NMR experiment 6). In this case, temperatures were monitored up to 98 °C.

A series of spectra acquired in NMR experiments 5 and 6 were similar to those recorded for native ns-LTP1, with the exception of much lower temperatures of denaturation (Figure S4 of the Supporting Information). The obtained integrated absolute value of the intensity difference Y_n and data reported previously (*12*) were fitted to eq 11 (**Figure 2** and **Table 1**). A reference temperature of 60 °C was used for calculating the $\Delta S^{\ddagger}$ denaturation barriers of reduced ns-LTP1b samples. It should be noted that the fitted values of $\Delta S^{\ddagger}$ represent formal quantities, including not only the activation entropy but also the accessibility of the cysteins to the reducing agent and concentration effects. The activation Gibbs free energies also depend on the concentration of the reducing agent. The activation enthalpy calculated using eq 10 from the comparison of transition temperatures and heating rates of NMR experiment 6 and those reported by Perrocheau et al. (*12*) was 86 kJ mol^{-1}. Note that the T_m difference, neglected in eq 10, was relatively large (16 K) in this case. A correction for the T_m difference provides $\Delta H^{\ddagger} = 88$ kJ mol^{-1}.

The supplier's user manual of the instrument used in this study recommends avoiding reducing agents in DSC measurements when possible. Nonreproducible baseline artifacts when using reducing agents such as dithiothreitol have been described in literature (*27*). However, some studies do not report any anomalies using dithiothreitol (*28*, *29*). To our knowledge, experimental DSC data using sodium metabisulfite have not yet been published, and on the basis of the current information, one cannot draw unambiguous conclusions regarding the compatibility of metabisulfites with the DSC experiment. Nevertheless, calorimetric curves of ns-LTP1b reduced with 10 mM sodium metabisulfite were recorded. Large and not well-reproducible negative peaks were observed at low temperatures in blank DSC runs with the buffer containing sodium metabisulfite, which makes interpretation of the DSC curves unreliable. The data obtained on the reduced ns-LTP1b sample exhibited some additional irregular changes of the heat capacity around 80 °C, indicating that thermal denaturation might occur at this temperature (data not shown), but they were not analyzed quantitatively.

The effect of another reducing agent, GSH, was also tested in NMR experiment 7. Native ns-LTP1b was heated to 60 °C, and GSH was added to a final concentration of 30 mM. The rate of denaturation, calculated from a series of NMR spectra, (1.9 ± 0.2) × 10^{-5} s^{-1}, was close to the denaturation rate of ns-LTP1 reduced by 2 mM metabisulfite calculated for the same temperature (1.2 × 10^{-5} s^{-1}). The calculated activation Gibbs free energy is presented in **Table 1**.

DISCUSSION

Thermal changes of extremely stable ns-LTP1b were studied in a wide range of temperatures including its denaturation above 100 °C. The ns-LTP1b structure changed within the limits of a well-folded protein and fully reversibly up to 100 °C, in agreement with similar results reported in the literature (*12*, *14*, *16*). The observed denaturation of ns-LTP1b was a highly cooperative transition, typical for small proteins. Cooling experiments supported by slow denaturation observed at 100 °C, just below the apparent transition temperature, revealed that the unfolding is irreversible. This finding is in a good agreement with results of Van Nierop et al. (*16*), who reported that ns-LTP1/ns-LTP1b samples incubated at various temperatures (96, 105, and 110 °C) differed in binding to monoclonal antinative and antifoam antibodies and in elution profiles on a reversed-phase chromatographic column. The denatured sample provided NMR spectra with the integral intensities comparable to native ns-LTP1b and DLS measurements confirmed the monomeric nature of the denatured sample. The major peaks observed in mass spectra corresponded to intact unmodified ns-LTP1 and to products of one and two deamidations. It is therefore unlikely that the irreversibility of the denaturation is a result of heavy chemical decomposition or aggregation of the unfolded species.

Irreversibility of the denaturation makes a thermodynamic analysis of the process irrelevant. Instead, a kinetic analysis (*18*, *20*) based on the transition state theory was applied to the denaturation data in this study. To evaluate the reliability of such an approach, results obtained at different experimental conditions will be discussed and compared to the data published previously.

The calorimetric curve was more asymmetric than expected for a single irreversible transition (*18*, *20*). The heat absorbed at lower temperatures was therefore attributed to events not directly related to the protein unfolding. The sharp and well-defined peak

at the highest temperature was interpreted as unfolding of the protein. Fitting the DSC data to models introduced to account for the asymmetric shape of the calorimetric curve is reviewed in **Table 2**. The best fit was obtained when the denaturation was combined with two irreversible transitions (model 5), but this should not be taken as an experimental determination of the nature of the heat consumption at low temperatures.

The kinetic model was sufficient to describe the NMR denaturation data with the correlation coefficients r^2 higher than 0.99. Apparent transition temperatures were obtained with a good precision in two NMR experiments with different heating rates (NMR experiments 2 and 3). Almost identical activation Gibbs energies, calculated for 105 °C, were derived from both experiments (117.7 and 117.8 kJ mol^{-1}). The obtained values were 1 kJ mol^{-1} lower than $\Delta G^{\ddagger} = 118.7$ kJ mol^{-1} calculated from previously reported results of incubation at the same temperature (*16*) and approximately 3 kJ mol^{-1} higher than $\Delta G^{\ddagger}$ values obtained from our DSC measurement (**Table 2**).

Three different ways of calculating activation enthalpy $\Delta H^{\ddagger}$ were tested: Approach 1, fitting a denaturation curve obtained in a single NMR experiment to eq 11; approach 2, calculating $\Delta H^{\ddagger}$ from denaturation temperatures T_m determined in two NMR experiments with different average heating rate; and approach 3, calculating $\Delta H^{\ddagger}$ from rates of denaturation during isothermal incubation at various temperatures (Arrhenius analysis based on eq 2).

Approach 1, that is, the method introduced in this study, provided a reliable estimate of $\Delta H^{\ddagger} = 191$ kJ mol^{-1}, close to the result from DSC models 4 and 5 (196 and 204 kJ mol^{-1}), when the region of temperatures close to T_m was sampled well (NMR experiment 3). On the other hand, partitioning the activation barrier $\Delta G^{\ddagger}$ into the enthalpic and entropic contributions failed in NMR experiment 2, where the transition region was sampled only sparsely. Approach 2, applied to denaturation temperatures T_m obtained from NMR experiments 2 and 3, and approach 3, applied to denaturation rates calculated from NMR experiment 4 and from the chromatographic results published by Van Nierop et al. (*16*), gave $\Delta H^{\ddagger}$ of 199 and 184 kJ mol^{-1}, respectively, in good agreement with the values derived from DSC and NMR experiment 3.

It can be concluded that a good agreement of the activation Gibbs energies, defining the denaturation rates, was obtained among all experimental conditions tested in this study and also in comparison with a previous report (*16*). Activation enthalpies close to the results of DSC where obtained from a single NMR experiment when the transition region of temperatures was sampled well (approach 1, NMR experiment 3) or by using T_m values from two different measurements (approach 2, NMR experiments 2 and 3). Estimation of the activation enthalpies allowed prediction of rate constants at lower temperatures. Accuracy of such extrapolations is given by the range of T_m values covered. The standard deviation of the activation enthalpies determined by different approaches may be used to estimate the expected error of the prediction at a particular temperature.

In agreement with the previous reports (*12*, *14*, *15*, *17*), the activation barrier $\Delta G^{\ddagger}$ of the ns-LTP1b thermal denaturation was found to be remarkably high. The factors stabilizing the ns-LTP1 structure have been discussed recently by Perrocheau et al. (*12*). These authors studied effects of glycation, of reducing the disulfide bonds, and of hydrolysis of the ester bond between the Asp 7 and the attached lipid. The most dramatic decrease of the heat stability was observed when disulfide bridges were reduced by metabisulfite. This reducing agent was chosen because it is widely used as an antioxidant in the food industry and is also produced by yeast.

The complete denaturation curves published in the literature under reducing conditions allowed us to compare our results with the previous report (*12*). The $\Delta G^{\ddagger}$ values obtained from ref *12* and from NMR experiment 5, performed at identical reducing conditions, were 107.6 and 106.6 kJ mol^{-1}, respectively. The $\Delta H^{\ddagger}$ values obtained by applying approach 1 to the data reported in literature (*12*) and by applying approach 2 to T_m derived from ref *12* and from NMR experiment 5 were also similar (89 and 88 kJ mol^{-1}, respectively). The higher $\Delta H^{\ddagger}$ obtained from NMR experiment 5 by approach 1 indicates that temperatures were not sampled well in the transition region, as discussed above. When the sampling was improved by lowering the metabisulfite concentration (NMR experiment 6), the $\Delta H^{\ddagger} = 119$ kJ mol^{-1} obtained by approach 1 fit the trend of lowering activation enthalpies by reducing disulfide bonds. The significant decrease of the denaturation activation enthalpy from ≈200 kJ mol^{-1} of the native ns-LTP1b to ≈120 kJ mol^{-1} at 2 mM bisulfite concentration and ≈90 kJ mol^{-1} at 10 mM bisulfite concentration lowers the denaturation activation barriers of the reduced samples.

It should be noted that the analysis of the methyl regions of the NMR spectra, applied in this study, reflects changes in the packing of the amino acid side chains, which are directly related to denaturation. On the contrary, circular dichroism (CD) in the far ultraviolet region, used by Perrocheau et al., reflects ordering of the protein backbone, which may be preserved during denaturation in some cases (*30*). Nevertheless, the $\Delta H^{\ddagger}$ and $\Delta G^{\ddagger}$ values obtained from NMR and CD data at identical reducing conditions were comparable.

Perrocheau et al. also found that free thiol groups are present already in ns-LTP1 isolated from malt (*12*). As metabisulfite is not used in the brewing process, Perrocheau et al. suggested that glutathione may play a role of an endogenous reducing agent (*12*). Therefore, the effect of GSH on ns-LTP1 denaturation was tested in this study as well. The results showed that rate of denaturation of ns-LTP1 treated with 30 mM GSH is comparable to the denaturation rate of ns-LTP1 reduced by 2 mM metabisulfite at the same temperature.

Other covalent modifications of ns-LTP1 studied by Perrocheau et al. included glycations and cleavage of the ester bond between the Asp7 and the oxylipin molecule. While the effect of glycations was negligible, the lipid modification contributed to the stability of ns-LTP1b. The stabilizing effect of the oxylipin was more pronounced in the reduced samples, where the apparent melting temperature was lower by 15 °C for ns-LTP1 as compared to ns-LTP1b. Similar comparison was more difficult to make for the nonreduced samples due to the incomplete denaturation curves, but the stabilizing effect did not exceed 5 °C.

The process of the ester bond cleavage was monitored in several studies. Lindorff-Larsen et al. found the ester bond to be stable at 37 °C and acidic conditions, having estimated the rate constant of the hydrolysis in the order of 10^{-8} to 10^{-7} s^{-1} at pH 4 (*6*), used in our study. Van Nierop et al. found that the ester bond cleavage is slow even at very high temperatures (*16*). Our analysis of their electrospray mass spectra provides a hydrolysis rate constant of 2×10^{-5} s^{-1} at 96 °C. These results show that most of the protein is likely to contain the lipid modification until the protein is unfolded at the heating rates used in our study (NMR experiments 2−6). The longer time scale of NMR experiment 1 allowed us to estimate the hydrolysis rate from our data. Fitting to the kinetic model (eq 3) provided a rate constant of 1.5×10^{-5} s^{-1} calculated for 96 °C. Our results thus are in agreement with previous reports.

Taking into account the ns-LTP1 impact on beer quality, the estimation of the transition state enthalpy and entropy presented above may lead to practical applications in food chemistry.

Calculated denaturation rate constants show that native ns-LTP1b is stable up to 60 °C (half-life in order of months), while the reduced protein denatures in a few hours at the same temperature. It demonstrates that the quality of barley products can alter at combinations of moderately elevated temperature and presence of reducing agents, with possible consequences for long-term storage. An even higher effect of reducing agents can be expected on processes involving heating, for example, brewing. Denaturation of ns-LTP1 can then influence beer foaming (*13*, *16*), which is an important quality parameter. After disulfide bond reduction with 10 mM sodium metabisulfite, the calculated half-life of ns-LTP1 decreases from 2 days to 20 min at 76 °C (typical temperature at the end of mashing) and from 60 to 2 min at 100 °C (temperature of wort boiling).

In conclusion, NMR and DSC provided complementary pictures of ns-LTP1b denaturation, the former reflecting structural changes showing up only when the protein unfolds and the latter monitoring heat changes during the whole process. The nature of the intermediates preceding unfolding cannot be directly derived from the presented data, but NMR spectra show that the protein structure does not change significantly up to temperatures close to T_m. The quantitative analysis of the data in terms of the transition state theory provided temperature-dependent denaturation rate constants as a simple measure of protein stability. Effects of reducing agents on ns-LTP1b thermal stability were studied, and their importance for quality of barley products was discussed.

ABBREVIATIONS USED

DSC, differential scanning calorimetry; GSH, reduced glutathione; ns-LTP1, lipid transfer protein 1; ns-LTP1b, covalently modified lipid transfer protein 1b (post-translational modification); NMR, nuclear magnetic resonance; MES, 4-morpholinoethanesulfonic acid; SDS-PAGE, sodium dodecylsulfate–polyacrylamide gel electrophoresis; MALDI-TOF MS, matrix-assisted laser desorption/ionization time-of-flight mass spectrometry; NOESY, nuclear Overhauser effect spectroscopy; DLS, dynamic light scattering; CD, circular dichroism.

ACKNOWLEDGMENT

We thank to Drs. Vladislav Kahle and Jan Lochman for technical help with the chromatography and Janette Bobál'ová and Pavel Řehulka for supervising J.Ž. after the death of J.C.

Supporting Information Available: Mass spectrum of fresh ns-LTP1b isolated from barley flour and of ns-LTP1b denatured in NMR experiment 2 (Figure S1), temperature chemical shift changes of well-resolved methyl signals (Figure S2), overlaid spectra taken in the course of heating already denatured (Figure S3) and reduced (Figure S4) ns-LTP1b. This material is available free of charge via the Internet at http://pubs.acs.org.

LITERATURE CITED

(1) Gorjanović, S. Barley grain non-specific lipid-transfer proteins (ns-LTPs) in beer production and quality. *J. Inst. Brew.* **2007**, *113*, 310–324.

(2) Heinemann, B.; Andersen, K. V.; Nielsen, P. R.; Bech, L. M.; Poulsen, F. M. Structure in solution of a four-helix lipid binding protein. *Protein Sci.* **1996**, *5*, 13–23.

(3) Lerche, M. H.; Kragelund, B. B.; Bech, L. M.; Poulsen, F. M. Barley lipid-transfer protein complexed with palmitoyl CoA: The structure reveals a hydrophobic binding site that can expand to fit both large and small lipid-like ligands. *Structure* **1997**, *5*, 291–306.

(4) Lerche, M. H.; Poulsen, F. H. Solution structure of barley lipid transfer protein complexed with palmitate. Two different binding modes of palmitate in the homologous maize and barley nonspecific lipid transfer proteins. *Protein Sci.* **1998**, *7*, 2490–2498.

(5) Douliez, J. P.; Jégou, S.; Pato, C.; Mollé, D.; Tran, V.; Marion, D. Binding of two mono-acylated lipid monomers by the barley lipid transfer protein, LTP1, as viewed by fluorescence, isothermal titration calorimetry and molecular modelling. *Eur. J. Biochem.* **2001**, *268*, 384–388.

(6) Lindorff-Larsen, K.; Lerche, M. H.; Poulsen, F. M.; Roepstorff, P.; Winther, J. R. Barley lipid transfer protein, LTP1, contains a new type of lipid-like post-translational modification. *J. Biol. Chem.* **2001**, *276*, 33547–33553.

(7) Douliez, J. P.; Jégou, S.; Pato, C.; Larré, C.; Mollé, D.; Marion, D. Identification of a new form of lipid transfer protein (LTP1) in wheat seeds. *J. Agric. Food Chem.* **2001**, *49*, 1805–1808.

(8) Bakan, B.; Hamberg, M.; Perrocheau, L.; Maume, D.; Rogniaux, H.; Tranquet, O.; Rondeau, C.; Blein, J.-P.; Ponchet, M.; Marion, D. Specific adduction of plant lipid transfer protein by an allene oxide generated by 9-lipoxygenase and allene oxide synthase. *J. Biol. Chem.* **2006**, *281*, 38981–38988.

(9) Gorjanović, S.; Sužnjević, D.; Beljanski, M.; Hranisavljević, J. Barley lipid-transfer protein as heavy metal scavenger. *Environ. Chem. Lett.* **2004**, *2*, 113–116.

(10) Gorjanović, S.; Beljanski, M. V.; Sužnjević, D. Electrochemical study of the lipid-transfer protein. *Electroanalysis* **2005**, *17*, 1861–1864.

(11) Gorjanović, S.; Spillner, E.; Beljanski, M. V.; Gorjanović, R.; Pavlović, M.; Gojgić-Cvijanović, G. Malting barley grain non-specific lipid-transfer protein (ns-LTP): Importance for grain protection. *J. Inst. Brew.* **2005**, *111*, 99–104.

(12) Perrocheau, L.; Bakan, B.; Boivin, P.; Marion, D. Stability of barley and malt lipid transfer protein 1 (LTP1) toward heating and reducing agents: Relationships with the brewing process. *J. Agric. Food Chem.* **2006**, *54*, 3108–3113.

(13) Sørensen, S. B.; Bech, L. M.; Muldbjerg, M.; Beenfeldt, T.; Breddam, K. Barley lipid transfer protein 1 is involved in beer foam formation. *MBAA Tech. Quart.* **1993**, *30*, 136–145.

(14) Lindorff-Larsen, K.; Winther, J. R. Surprisingly high stability of barley lipid transfer protein, LTP1, towards denaturant, heat and proteases. *FEBS Lett.* **2001**, *488*, 145–148.

(15) Jégou, S.; Douliez, J. P.; Mollé, D.; Boivin, P.; Marion, D. Evidence of the glycation and denaturation of LTP1 during the malting and brewing process. *J. Agric. Food Chem.* **2001**, *49*, 4942–4949.

(16) Van Nierop, S. N. E.; Evans, D. E.; Axcell, B. C.; Cantrell, I. C.; Rautenbach, M. Impact of different wort boiling temperatures on the beer foam stabilizing properties of lipid transfer protein 1. *J. Agric. Food Chem.* **2004**, *52*, 3120–3129.

(17) Perrocheau, L.; Rogniaux, H.; Boivin, P.; Marion, D. Probing heat-stable water-soluble proteins from barley to malt and beer. *Proteomics* **2005**, *5*, 2849–2858.

(18) Zhadan, G. G.; Shnyrov, V. L. Differential-scanning-calorimetric study of the irreversible thermal denaturation of 8 kDa cytotoxin from the sea anemone *Radianthus macrodactylus*. *Biochem. J.* **1994**, *299*, 731–733.

(19) Finkelstein, A. V.; Ptitsyn, O. B. *Protein Physics: A Course of Lectures*; Academic Press: London, 2002.

(20) Sánchez-Ruiz, J. M.; López-Lacomba, J. L.; Cortijo, M.; Mateo, P. L. Differential scanning calorimetry of the irreversible thermal denaturation of thermolysin. *Biochemistry* **1988**, *27*, 1648–1652.

(21) Fersht, A. *Structure and Mechanism in Protein Science: A Guide to Enzyme Catalysis and Protein Folding*; W. H. Freeman and Co.: New York, 1999.

(22) Delaglio, F.; Grzesiek, S.; Vuister, G. W.; Zhu, G.; Pfeifer, J.; Bax, A. NMRPipe—A multidimensional spectral processing system based on Unix pipes. *J. Biomol. NMR* **1995**, *6*, 277–293.

(23) Markley, J. L.; Bax, A.; Arata, Y.; Hilbers, C. W.; Kaptein, R.; Sykes, B. D.; Wright, P. E.; Wuthrich, K. Recommendations for the presentation of NMR structures of proteins and nucleic acids - IUPAC-IUBMB-IUPAB Inter-Union Task Group on the Standardization of Data Bases of Protein and Nucleic Acid Structures Determined by NMR Spectroscopy. *J. Biomol. NMR* **1998**, *12*, 1–23.

(24) Kumar, A.; Wagner, G.; Ernst, R. R.; Wüthrich, K. Buildup rates of the nuclear Overhauser effect measured by two-dimensional proton magnetic resonance spectroscopy: Implications for studies of protein conformation. *J. Am. Chem. Soc.* **1981**, *103*, 3654–3658.

(25) Jégou, S.; Douliez, J. P.; Mollé, D.; Boivin, P.; Marion, D. Purification and structural characterization of LTP1 polypeptides from beer. *J. Agric. Food Chem.* **2000**, *48*, 5023–5029.

(26) Baxter, N. J.; Williamson, M. P. Temperature dependence of ^{1}H chemical shifts in proteins. *J. Biomol. NMR* **1997**, *9*, 359–369.

(27) Suurkuusk, M.; Hallen, D. Denaturation of apolipoprotein A-I and the monomer form of apolipoprotein A-I-Milano. *Eur. J. Biochem.* **1999**, *265*, 346–352.

(28) Ang, H. C.; Joerger, A. C.; Mayer, S.; Fersht, A. R. Effects of common cancer mutations on stability and DNA binding of full-length p53 compared with isolated core domains. *J. Biol. Chem.* **2006**, *281*, 21934–21941.

(29) Tang, C.-H. Thermal denaturation and gelation of vicilin-rich protein isolates from three *Phaseolus legumes*: A comparative study. *LWT-Food Sci. Technol.* **2008**, *41*, 1380–1388.

(30) Dolgikh, D. A.; Abaturov, L. V.; Bolotina, I. A.; Brazhnikov, E. V.; Bychkova, V. E.; Gilmanshin, R. I.; Lebedev, Y. O.; Semisotnov, G. V.; Tiktopulo, E. I.; Ptitsyn, O. B. Compact state of a protein molecule with pronounced small-scale mobility—Bovine α-lactalbumin. *Eur. Biophys. J.* **1985**, *13*, 109–121.

Received December 10, 2008. Revised manuscript received August 11, 2009. Accepted August 11, 2009. This work was supported by the Grants 1M0570 (J.Ž. and J.C.), MSM0021622413 (M.M., L.Ž., and M.W.), and LC06030 (V.S.) of the Ministry of Education, Youth, and Physical Culture of the Czech Republic and by Grant AV0Z40310501 of the Academy of Sciences of the Czech Republic (J.Ž. and J.C.).